# Novel Pattern Transition Scenarios in Electroconvection in Homeotropic Nematics under Magnetic Field (Mathematical Aspects of Complex Fluids)

AUTHOR(S):

Huh, Jong-Hoon; Hidaka, Yoshiki; Kai, Shoichi

数理解析研究所講究録
1081 巻 1999 年 10-18



# Novel Pattern Transition Scenarios in Electroconvection in Homeotropic Nematics under Magnetic Field

Jong-Hoon Huh, Yoshiki Hidaka and Shoichi Kai
Department of Applied Physics, Faculty of Engineering,
Kyushu University, Fukuoka 812-8581, Japan

We report a new transition scenario from a uniform state to the spatio-temporal chaos (STC) for the electroconvection in the homeotropically aligned nematics, in which a magnetic field is applied perpendicularly to the electric field. Above the Lifshitz frequency $f_L$ the amplitude of the electric field increasing, a stationary periodic rolls state becomes unstable, then evolves to STC-I (i.e., the defect chaos) at a certain electric field. At a higher electric field, the second stationary periodic rolls (i.e., abnormal rolls) are also found above a characteristic intensity of the magnetic field $H^*$. At further higher electric field the second stationary periodic rolls state becomes unstable again, then evolves to more complicated STC (STC-II). Above $H^*$ the abnormal rolls instability corresponding to an azimuthal rotation of the director plays key roles on the pattern transitions between stationary and non-stationary states as well as between the two stationary ones. Based on the systematic study, a clear phase diagram was determined in the $H$- $\varepsilon$ plane. These results are remarkably different from ones below $f_L$ previously reported.

## Introduction

AC-driving electroconvection in nematic liquid crystals supplies attractive pattern formations far from equilibrium system, in which chaotic structures as well as periodic ones are found with increasing voltage. The transition scenario from a uniform state to spatio-temporal complex states due to secondary instabilities has been studied for understanding nonequilibrium systems[1-5]. Electroconvection in liquid crystals sandwiched between two electrodes (defined as the $xy$-plane) is induced by the periodical focusing of the electric charges, for which a unit director $\mathbf{n} = (n_x, n_y, n_z)$ defined as the locally averaged orientation of rod-like molecules plays main roles on the convection[6-7].

In the planar geometry ( $\mathbf{n} = (1, 0, 0)$ in the initial state), the scenario based on the electrohydrodynamic instabilities has been intensively investigated by both

theorists and experimentalists[2-4,8]. In general the spatio-temporal chaos (STC) called the defect chaos (i.e., fluctuating Williams domain) has been found in the planar geometry[8]. On the other hand, in the homeotropic geometry ( **n** = (0, 0, 1) in the initial state) with no magnetic field, it was recently found that a new type of STC is directly induced at onset *via* a supercritical bifurcation in both experimental[9,10] and theoretical researches[5,11,12]. We have called this STC the soft-mode turbulence (SMT).

The physical mechanism of SMT at high frequency, i.e., above a characteristic frequency $f_L$ could be understood as nonlinear couplings between a convection mode and additional Goldstone mode corresponding to infinitely-degenerated rotation of the director[11,12]. The Goldstone mode must be induced by a continuously rotational symmetry-breaking due to the bend Freedericksz transition of the director before the convection is induced.

We have been investigating the pattern changes of SMT and their spatial-temporal properties under superimposing magnetic field which can suppress the additional Goldstone mode, i.e., the azimuthally-free rotation of the director **n**[10,13,14]. Notice that the director **n** in nematics with diamagnetic anisotropy $\chi_a > 0$ tends to parallel to a magnetic field[6,7]. Meanwhile, the electroconvection in homeotropic system under a magnetic field shows two types of primary patterns with respect to the frequency of the applied AC-voltage. In general, one can observe normal rolls (NR) with wavevector **k** of the convection rolls parallel to the applied magnetic field (the $x$-axis) above the Lifshitz frequency $f_L$, and oblique rolls (OR) with a certain angle between **k** and the $x$-axis below $f_L$, respectively[12].

In this report, we have focused on the electroconvection at a high frequency ($f > f_L$) of the applied voltage corresponding to the normal rolls regime[12]. In the normal rolls regime, we have found a new restabilized stationary periodic state at greater voltages than those for STC. This new stationary state turns out to be *abnormal rolls* (AR), which is recently known as a homogeneous azimuthal rotation of the director **n** in the $xy$-plane due to nonlinear couplings between the flow field and the director field in nematics[15-17]. We will show interesting results on a scenario from a stationary state to STC in the normal rolls regime ($f > f_L$), which are first found in the homeotropic system under a constant magnetic

field, and compare with the previous results investigated in the oblique rolls regime ($f < f_L$)[18].

## Experiment

The *p*-methoxybenzilidene-*p'*-*n*-butylaniline (MBBA) is used as a typical nematic liquid crystal for the electroconvection, which is filled between two parallel glass plates whose surfaces are coated with transparent electrodes, indium tin oxide (ITO). The distance $d$ = 52 $\mu$ m between the glass plates is maintained with polymer spacer and the lateral size of a cell is $1 \times 1$ cm$^2$. In order to achieve the homeotropic alignment, the surface of the glass plates is treated by surfactant *n-n'*-dimethy-*n*-octadecyl-3-aminopropyl-trimethoxy silyl chloride (DMOAP). The conductivities of MBBA are $\sigma_{\parallel} = 5.07 \times 10^{-7}\ \Omega^{-1}$/m and $\sigma_{\perp} = 3.47 \times 10^{-7}\ \Omega^{-1}$/m, respectively, which are controlled by 0.01 *wt.%* doping of tetra-*n*-butyle-ammonium bromide (TBAB), and the dielectric constants are $\varepsilon_{\parallel} = 4.40$ and $\varepsilon_{\perp} = 5.23$, respectively. In all measurements the temperature of the cell is controlled at 30 $\pm$ 0.01 ℃ with a control stage and a copper cavity wrapped by the polytetrafluoroethylene (Teflon). A constant magnetic field is applied parallel to the glass plates ( $\mathbf{H} = (H_x, 0, 0)$ ) and the frequency of the applied voltages is fixed at 2000 Hz, which is applicable to the each applied magnetic intensity for achieving the normal rolls regime in our experiment.

A measurement for pattern dynamics was done in the following procedure. Under a constant magnetic field $H$, an applied voltage was first raised to 6.00 V between $V_F(H)$ and $V_c(H)$ for maintaining the Freedericksz deformation, where $V_F(H)$ is a threshold for Freedericksz deformation at $H$ and $V_c(H)$ a critical voltage for convection at $H$, respectively. After the uniform steady state of the Freedericksz deformation had been achieved (typically for 10 minutes), the applied voltage was raised to a desired value $V_F(H)$ greater than $V_c(H)$ in order to get the convection. After waiting for enough time to finish its transient state, the pattern dynamics was taken by the CCD camera and recorded onto a video tape. Raising voltage from $V_F(H)$ to $V_2(H)$, we carried out the next measurement for the higher value $V_2(H)$. The measurements were done for selected values $V_{i\ (i = 1, 2, \ldots)} > V_c$ at a constant intensity of $H$. The intensity of $H$ being changed, a

series of measurement was repeated with the same procedures.

We analyzed the experimental data in order to investigate the pattern dynamics as follows. First, one hundred-pieces of two-dimensional image with the size of 256 × 256 pixels and the brightness of 256 gray values were sampled from video images by using a computer (Power Macintosh), the image-capturing board (Scion LG-3) and the software NIH Image. Since the size of 1-pixel $\Delta x$ ( = $\Delta y$) was 2.3 $\mu$ m, the whole image size was 590 × 590 $\mu$ m$^2$. The time series $I_i(t)$ was obtained at each point $(x_i, y_i)_{(i = 1,2,\ldots,1000)}$ randomly selected in each image. The temporal autocorrelation function $C_i(t)$ was calculated from the time series $I_i(t)$. Then we obtained an averaged autocorrelation function $C_{av}(t)$ (= $\langle C_i(t) \rangle_i$). The correlation time $\tau$ of pattern fluctuations was obtained with respect to a normalized control parameter $\varepsilon = (V^2 - V_c^2)/V_c^2$ by fitting the function $C_{av}(t)$ to $C(0)\ exp(-t / \tau)$ using least-squares regression, as shown in the inset of Fig.1.

## Results and Discussion

Figure 1 shows a dependence of the relaxation frequency $\tau^{-1}$ of pattern fluctuations on $\varepsilon$ for various constant magnetic intensities. The two different be-

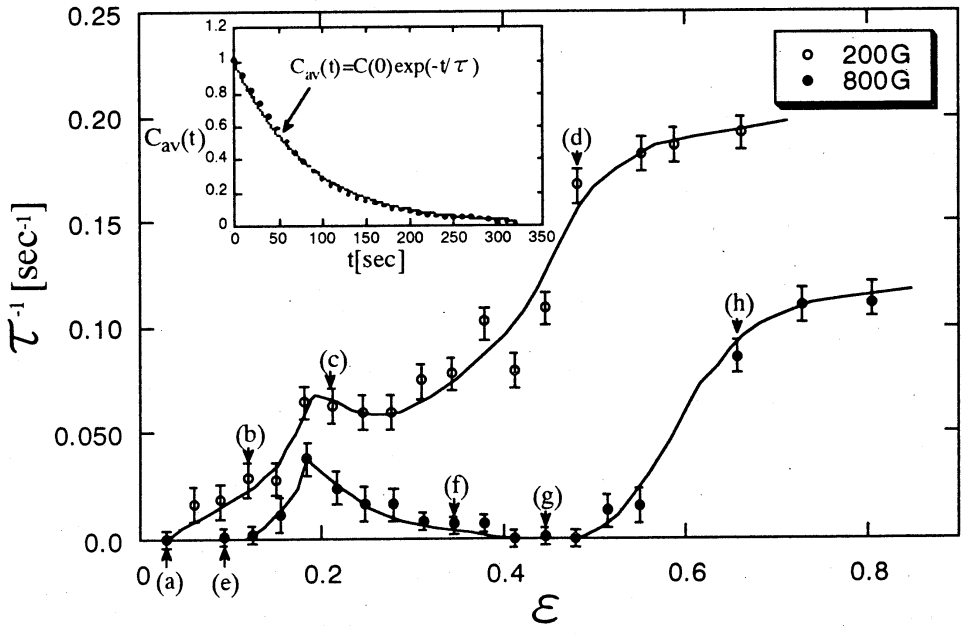


**FIGURE 1** Dependence of the relaxation frequency $\tau^{-1}$ of pattern fluctuations on the normalized control parameter $\varepsilon$ under each constant magnetic field. Two types of different behavior are shown for $H$ = 200 G and 800 G. The solid lines are eye-guide lines.

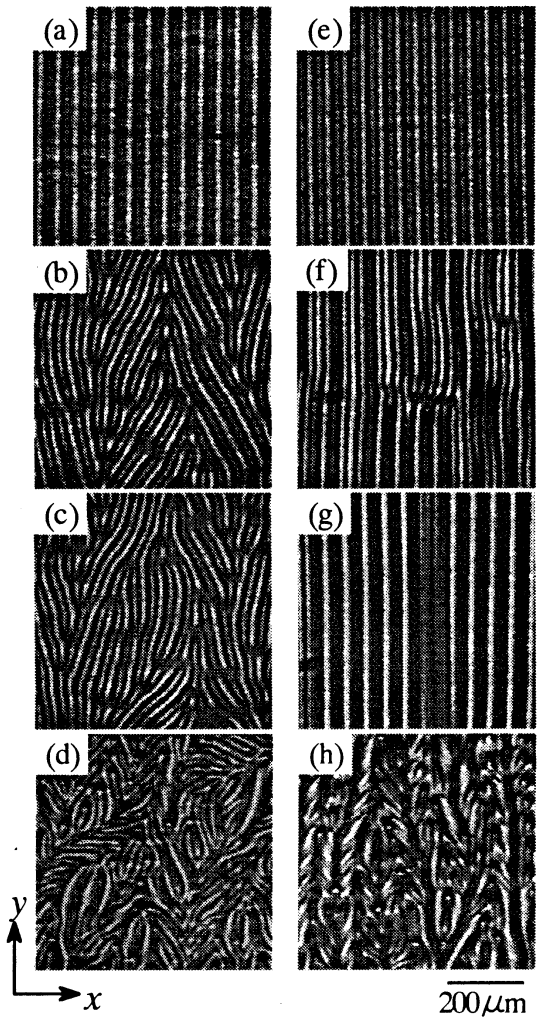


**FIGURE 2** Real pattern images under each constant magnetic field. (a) - (d) are typical patterns observed for the normalized control parameter $\varepsilon$ at $H$ = 200 G ((a) $\varepsilon$ = 0.029, (b) $\varepsilon$ = 0.12, (c) $\varepsilon$ = 0.21, and (d) $\varepsilon$ = 0.48). (e) - (h) are also at $H$ = 800 G ((e) $\varepsilon$ = 0.094, (f) $\varepsilon$ = 0.34, (g) $\varepsilon$ = 0.44, and (h) $\varepsilon$ = 0.66).

havior of $\tau^{-1}$ ( $\varepsilon$ ) with respect to the magnetic intensity $H$ can be observed, *e.g.*, $H$ = 200 G and $H$ = 800 G, respectively. At $H$ = 200 G, a stationary rolls state ( $\tau^{-1}$ = 0) is maintained until $\varepsilon$ reaches to $\varepsilon \sim 0.03$ ( (a) ) shown in Fig.1, then becomes unstable and evolves to STC ( $\tau^{-1} \neq 0$) for $\varepsilon >$ 0.03. At $H$ = 800 G, on the other hand, although a stationary rolls state ( $\tau^{-1}$ = 0) becomes unstable and evolves to STC ( $\tau^{-1} \neq 0$) beyond $\varepsilon \sim 0.13$, the second stationary state ( $\tau^{-1}$ = 0) appears again at $0.4 < \varepsilon < 0.5$ ((g)) indicating a maximum value of $\tau^{-1}$ at $\varepsilon \sim 0.18$. Then the second stationary state becomes unstable and evolves to STC ( $\tau^{-1} \neq 0$) beyond $\varepsilon \sim 0.5$.

In order to understand the behavior of these pattern dynamics more clearly, we show the corresponding real images in Fig.2. Figure 2(a) - (d) are typical patterns observed at $H$ = 200 G with increasing $\varepsilon$ , and Fig.2(e) - (h) at $H$ = 800 G. At 200 G, the stationary periodic rolls state shown in Fig.2(a) becomes unstable and evolves to STC ((b) and (c)), and then to the more complicated state (d) increasing applied voltage. At 800 G, on the other hand, the stationary periodic rolls state (e) becomes unstable and evolves to STC (f). However, further increasing the voltage, the second stationary periodic rolls state (g) again appears, and then evolves to a more complicated state (h) with higher voltages. The second stationary state (g) at 800 G turns out to be the abnormal rolls (AR)[15,16,18], which was also named the reentrant normal rolls in our previ-

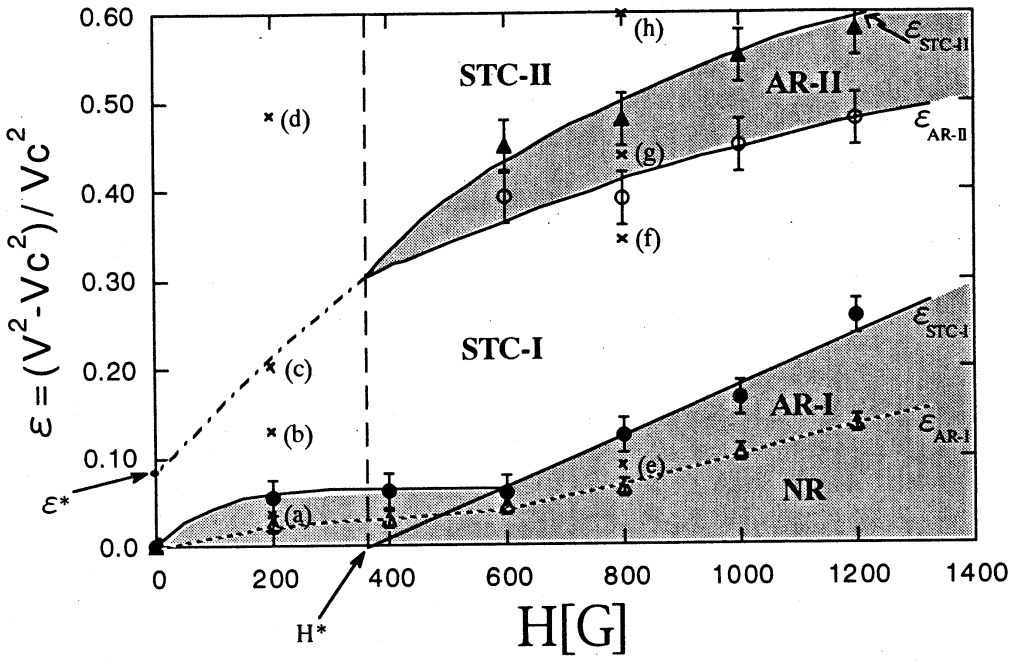


**FIGURE 3** Phase diagram in the $H$ - $\varepsilon$ plane. All data with error bars except open triangles on the dot-line $\varepsilon_{AR\text{-}I}$ were obtained from the dependencies of $\tau^{-1}$ on $\varepsilon$ by calculating temporal autocorrelation functions for various magnetic fields (See Fig.1 and the text). All solid lines were drawn by the eye-guide. The dot-line $\varepsilon_{AR\text{-}I}$ was determined under the cross-polarized set. The two shadow regions represent the stationary states ($\tau^{-1} = 0$), and the rest does the spatio-temporal chaotic states ($\tau^{-1} \neq 0$), respectively. All points (a) - (h) marked by × correspond ones in Figs.1, 2. See the text for details.

ous report[13]. In order to investigate the director field of AR, we have inserted a cross-polarized set into the standard optical set. The cross-polarized set can be rotated around the $z$-axis. Under our revised optical set, AR with a finite azimuthal rotation angle $\alpha$ of the director **n** can be discriminated from the conventional normal rolls. We have always checked under the optical set whether the pattern is AR or not.

Figure 3 shows a phase diagram in the $H$ - $\varepsilon$ plane. The two shadow regions represent the stationary rolls states, and the rest does STC. Owing to $H$ which can stabilize the director **n**, both the critical voltage $V_c(H)$ for convection and the threshold voltage $V_{STC}(H)$ (i.e., $\varepsilon_{STC}(H)$) for STC are expected to increase with increasing $H$. Similarly to previous reports[10,14], $V_c(H)$ monotonously increased in proportion to $H^2$ (not shown in Fig.3). However, it seems that the threshold $\varepsilon_{STC\text{-}I}(H)$ for STC-I shows a peculiar dependence with two steps on $H$. In other words, $H$ increasing, $\varepsilon_{STC\text{-}I}(H)$ shows small increment below $H$ =

600 G, and large one beyond 600 G. Therefore, we could define a threshold intensity of magnetic field $H^*$ as 350 G by the extrapolation of $\varepsilon_{STC\text{-}I}(H)$ with a linear slope on $H$[14].

Now, labeling (a) - (h) marked by × in Fig.3 correspond to ones in Fig.1 and 2. It is worth noting that the second stationary rolls at (g) in Fig.3 are AR (described as AR-II in Fig.3) which can be characterized by $\tau^{-1} = 0$ and $\alpha \neq 0$. Below STC-I state, moreover, there exist two different rolls states, that is, a stationary state of normal rolls (NR) at $\varepsilon(H) < \varepsilon_{AR\text{-}I}(H)$ and the other stationary state (AR-I) at $\varepsilon(H) > \varepsilon_{AR\text{-}I}(H)$. Here $\varepsilon_{AR\text{-}I}(H)$ (the dotted-line) indicates the threshold for AR. There are two different ARs, i.e., AR-I ((a) and (e)) and AR-II ((g)). The AR with small $\alpha$ at small $\varepsilon$ ( $\varepsilon_{AR\text{-}I} < \varepsilon < \varepsilon_{STC\text{-}I}$) is called AR-I, and the AR with large $\alpha$ at large $\varepsilon$ ( $\varepsilon_{AR\text{-}II} < \varepsilon < \varepsilon_{STC\text{-}II}$) AR-II. In addition, from the phase diagram in Fig.3 the two stationary regions (shadow regions) would be expected to be unified into one region (i.e., $\varepsilon_{STC\text{-}I} = \varepsilon_{STC\text{-}II}$) in the sufficiently strong magnetic fields (not shown in Fig.3). Therefore we have checked it at $H$ = 2000 G, and found that no STC-I exists between AR-I and AR-II. Therefore another new threshold $H^+$ could be defined.

Below $H^*$ the second stationary rolls have not been found. However, an strange transition (around the dash-dotted line at $0 < H < H^*$) for pattern dynamics due to the abnormal rolls instability may exist, although we have not perfectly determined the threshold line. Extrapolating this transition line into $H = 0$, it intersects at $\varepsilon^* \sim 0.1$. This value coincides with a transition point from a slow dynamics to a fast one, which was found in the soft-mode turbulence in our previous report[9]. We proposed that it may be related to the AR-instability. The further study for understanding the unknown transition at $0 < H < H^*$ is in progress.

Finally, it is worth comparing the present results in the normal rolls regime with the results in the oblique rolls one previously reported[14]. The behavior of the threshold $\varepsilon_{STC\text{-}I}(H)$ for STC-I is similar to the previous report. That is, it shows two different slopes depending on $H$ in the $H$ - $\varepsilon$ plane and a characteristic magnetic field $H^*$ exists. However, there exists a remarkably different characteristic in the normal rolls regime. Namely, above $H^*$ no second stationary state like AR-II has been found in the oblique rolls regime. This means that in the oblique rolls regime STC-I can not be restabilized into the second stationary

state by the homogeneous rotation of the director due to the abnormal rolls instability. The result in the oblique rolls regime may be understood from the mechanism such that an uncompensated torque between the vector $\mathbf{C} = (n_x, n_y)$ and the wavevector **k** exists for STC[11,14]. In the oblique rolls regime, therefore, no second stationary state like AR-II appears beyond STC-I with increasing $\varepsilon$, because STC-I with the uncompensated torque always overcomes the restabilizing forces due to the homogeneous rotation of the director.

## Summary

In conclusions, we have carried out the systematic investigation for the electroconvection in the homeotropically aligned nematics under a constant mangetic field. In the normal rolls regime, we have found a new scenario from a uniform conductive state to STC under superimposing magnetic field, which is different from the previous results in the oblique rolls regime. Under a certain constant magnetic field ($H^* < H < H^+$) the applied voltage increasing, the second stationary state has been found beyond STC which was followed by the first stationary one. We could make it clear that the new scenario was strongly related with the abnormal rolls induced by the homogeneously azimuthal rotation of the director due to nonlinear couplings between the flow and the director field in nematics. Based on the present results, we are now trying to understand the dynamical properties of SMT in the normal rolls regime in the absence of magnetic field. The present study has supplied the very important hint for future progress.

### Acknowledgment

This work has been partly supported by a Grant-in-Aid for Scientific Research from the Ministry of Education, Science, Sports and Culture in Japan (No.08454107 and No.10440117).

### References

[1.] M. C. Cross and P. C. Hohenberg, Rev. Mod. Phys., **60**, 851 (1993).

[2.] S. Kai, H. Yamazaki, M. Araoka, and K. Hirakawa, J. Phys. Soc. Jpn., **41**, 1439 (1976).

[3.] I. Rehberg, S. Rasenat, V. Steinberg, Phys. Rev. Lett., **62**, 756 (1989).

[4.] S. Nasuno, O. Sasaki, and S. Kai, Phys. Rev. A, **46**, 4954 (1992).

[5.] L. Kramer, A. Hertrich and A. Pesch, *Pattern Formation in Complex Dissipative Systems*, edited by S. Kai (World Scientific, Singapore, 1992), p.238.

[6.] L. M. Blinov, *Electro-optical and magneto-optical properties of liquid crystals* (The Universities Press (Belfast) Ltd., Northern Ireland, 1983).

[7.] P. G. de Gennes and J. Prost, *The Physics of Liquid Crystals* (Oxford University Press, New York, 1993) 2nd ed.

[8.] S. Kai, and W. Zimmermann, Prog. Theor. Phys. Supp. No.**99**, 458 (1989).

[9.] Y. Hidaka, J. -H. Huh, K. Hayashi, M. I. Tribelsky and S. Kai, Phys. Rev., E **56**, R 6256 (1997).

[10.] H. Richter, N. Klopper, A. Hertrich and A. Buka, Europhys. Lett., **30**, 37 (1995).

[11.] A. G. Rossberg, A. Hertrich, L. Kramer and W. Pesch, Phys. Rev. Lett., **76**, 4729 (1996).

[12.] A. Hertrich, W. Decker, W. Pesch and L. Kramer, J. Phys. II 2, 1915 (1992).

[13.] S. Kai, K. Hayashi and Y. Hidaka, J. Phys. Chem., **100**, 19007 (1996).

[14.] J. -H. Huh, Y. Hidaka, and S. Kai, J. Phys. Soc. Jpn., **67**, 1948 (1998).

[15.] H. Richter, A. Buka and I. Rehberg, *Spatio-Temporal Patterns in Nonequilibrium Complex Systems*, Eds. P. Cladis and P. Palffy-Muhoray (Addison-Wesley, 1994) p.343; H. Richter, A. Buka and I. Rehberg, Mol. Cryst. Liq. Cryst., **251**, 181 (1994); H. Richter, A. Buka and I. Rehberg, Phys.Rev.E, **51**, 5886 (1995).

[16.] E. Plaut, W. Decker, A. G. Rossberg, L. Kramer, W. Pesch, A. Belaidi and R. Ribotta, Phys. Rev. Lett., **79**, 2367 (1997).

[17.] E. Plaut, and R. Ribotta, Phys. Rev. E, **56**, R2375 (1997).

[18.] J. -H. Huh, Y. Hidaka, and S. Kai, Phys. Rev. E **58**, 7355 (1998).